

Dissipation enhancement due to a single vortex reconnection in superfluid helium

R. Hänninen

O.V. Lounasmaa Laboratory, Aalto University, P.O. BOX 15100, 00076 AALTO, Finland

(Dated: March 27, 2013)

We investigate a single vortex reconnection event in superfluid helium at finite temperatures by using the vortex filament model. After the reconnection Kelvin waves are induced on vortices which strongly increase the energy dissipation. We evaluate this extra mutual friction dissipation and show that the dissipation power has a universal form which can be obtained when scaling the time (measured from the reconnection event) and the power by the mutual friction parameter α . This observation indicates that the Kelvin-wave cascade is not important in the energy dissipation process, at least within the parameter range used here, e.g. $\alpha \gtrsim 10^{-3}$. More importantly, even if the Kelvin waves greatly enhance the energy dissipation after reconnection, no change is seen in the angular momentum dissipation. This would explain why, at low temperatures, we need two effective dissipation coefficients: one for the energy and one for the momentum. This is observed in experiments on vortex front where the rotational motion of the front decouples from the external rotation reference frame. Our results also confirm the previous observations that the minimum distance between vortices scales approximately like $d \propto \sqrt{|t - t_{\text{rec}}|}$, both before and after the reconnection event. The prefactor is somewhat larger after the reconnection, simply due to larger curvatures appearing on the vortex.

I. INTRODUCTION

Energy dissipation in the zero temperature limit is an essential question in the field of quantum turbulence¹⁻⁴. Without quantized vortices helium superfluids would behave like an ideal Eulerian fluid. With zero viscosity turbulent boundary layer would not be formed and the fluid would exert no drag on particles. However, appearance of quantized vortices will break this ideal behavior and, in many cases, the superfluid behaves quasi-classically, similar to classical viscous fluids. In classical fluids the energy dissipation is due to viscosity. However, in superfluid helium (⁴He-II) the energy sink in the zero temperature limit is expected to be acoustic and appearing by phonon emission. In quantum fluids the vorticity is quantized in units of circulation quantum, and therefore the classical Kolmogorov-Richardson type cascade can only work down to scales of order the intervortex distance. At smaller scales the Kelvin-wave cascade is expected to be the dominant dissipation, transferring the energy to scales where it can be eventually dissipated by emission of phonons^{1,5-7}.

Reconnections are expected to play an important role in the energy cascade process, especially at scales or order intervortex distance, where the reconnections transfer the energy from the three dimensional hydrodynamic motion to one dimensional Kelvin waves along vortices¹. Reconnections also allow the system to be driven into a non-equilibrium steady state⁸. Also, a reconnection of two almost anti-parallel vortices has been shown to initialize a cascade of vortex loop generation^{1,9}, and this was argued to be the dominant dissipation mechanism for sparse tangle in the low temperature limit⁹.

At not too low temperatures the mutual friction (m.f.) dissipation is the dominant dissipation method which originates from scattering of quasiparticles from the vortex cores. At a reconnection event a vortex becomes strongly distorted and locally large velocities appear on the curved vortex, resulting that the mutual friction dissipation is strongly increased. This motivated us to evaluate the extra dissipation induced by a single reconnection event using the vortex filament model.

Our intention is not to try to evaluate the energy loss coming from the microscopic reconnection event. This is beyond the scope of the vortex filament model. Rather we try to evaluate how much the mutual friction dissipation is increased due to a single reconnection event. This may overestimate the dissipation occurring in complicate tangles where reconnections are frequent and there is not enough time for the m.f. to dissipate all energy, before the next reconnection occurs. This becomes more pronounced at low temperatures where the decay time increases. However, as shown below, the reconnections increase the energy dissipation but no change is seen in the angular momentum dissipation. This observation should be valid more generally in case of vortex tangles.

II. MODEL AND EQUATIONS

Our calculations are based on the vortex filament model¹⁰, where all the characteristic scales are assumed to be much larger than the vortex coresize, a_0 . In superfluid ⁴He the coresize is only of order 0.1 nm and a vortex can be considered to be thin (line vortex). Within the vortex filament model (VFM) the superfluid velocity, \mathbf{v}_s is simply given by the Biot-Savart law. At zero temperature the only force felt by the vortex, moving at velocity \mathbf{v}_L , is the classical Magnus force (per unit length), which is given by $\mathbf{f}_M = \kappa \rho_s (\mathbf{v}_s - \mathbf{v}_L) \times \hat{\mathbf{s}}'$, where $\hat{\mathbf{s}}'$ is the direction of the unit tangent at point \mathbf{s} on the vortex. Term $\kappa = \hbar/m_4 = 0.0997 \text{ mm}^2/\text{s}$ is the circulation quantum for superfluid ⁴He. Since the mass of the vortex core can typically be neglected, every point on the vortex simply moves at a local superfluid velocity

$$\mathbf{v}_s = \frac{\kappa}{4\pi} \hat{\mathbf{s}}' \times \mathbf{s}'' \ln \left(\frac{2\sqrt{l_+ l_-}}{e^{1/2} a_0} \right) + \frac{\kappa}{4\pi} \int' \frac{(\mathbf{s}_1 - \mathbf{s}) \times d\mathbf{s}_1}{|\mathbf{s}_1 - \mathbf{s}|^3}. \quad (1)$$

As done by Schwarz¹⁰, we have removed singularity that appears in the Biot-Savart integral, when trying to evaluate the superfluid velocity at some vortex point \mathbf{s} , by introducing the local term (first term on the r.h.s). Terms l_{\pm} are the lengths of

the line segments connected to \mathbf{s} after discretization, and the remaining line-integral is over the other segments, not connected to \mathbf{s} . Term \mathbf{s}'' , where the derivation is with respect to arclength, ξ , is the normal at \mathbf{s} .

At finite temperatures vortex motion couples with the motion of the normal component. The mutual friction force (per unit length) felt by a vortex is given by

$$\mathbf{f}_{\text{mf}}/\rho_s \kappa = \alpha \hat{\mathbf{s}}' \times \hat{\mathbf{s}}' \times (\mathbf{v}_s - \mathbf{v}_n) + \alpha' \hat{\mathbf{s}}' \times (\mathbf{v}_s - \mathbf{v}_n), \quad (2)$$

where α and α' are temperature and pressure dependent mutual friction coefficients, whose values are rather well known, both in superfluid ^4He and $^3\text{He-B}$. (Note that the results for this paper are calculated when $\alpha' = 0$). This results that at finite temperatures the velocity of vortex point is given by

$$\mathbf{v}_L = \mathbf{v}_s + \alpha \hat{\mathbf{s}}' \times (\mathbf{v}_n - \mathbf{v}_s) - \alpha' \hat{\mathbf{s}}' \times \hat{\mathbf{s}}' \times (\mathbf{v}_n - \mathbf{v}_s). \quad (3)$$

The power dissipated due to mutual friction can be calculated as:

$$P_{\text{mf}} = \int (\mathbf{v}_L \cdot \mathbf{f}_{\text{mf}}) d\xi = - \int (\mathbf{v}_L \cdot \mathbf{f}_M) d\xi \quad (4)$$

If we assume that normal fluid is at rest, $\mathbf{v}_n = 0$, then eventually one obtains that

$$P_{\text{mf}} = -\alpha \rho_s \kappa \int |\hat{\mathbf{s}}' \times \mathbf{v}_s|^2 d\xi \quad (5)$$

The negative sign, which is typically omitted below, only indicates that the energy is dissipated. Since the mutual friction dissipation is the only dissipation considered here (in addition to numerical dissipation), the dissipation power could also be calculated from the time derivate of the kinetic energy for the superfluid component. However, the time fluctuations at low m.f. dissipation complicate the calculation of the derivate. Therefore, we prefer to calculate P_{mf} using Eq. (5). Results, if using the energy, are very similar. In calculating the energy (E), momentum (P), and angular momentum (A) we may use line integral formulas¹¹:

$$\begin{aligned} E &= \rho_s \kappa \oint \mathbf{v}_s \cdot \mathbf{s} \times \hat{\mathbf{s}}' d\xi \\ \mathbf{P} &= \rho_s \kappa \oint \mathbf{s} \times \hat{\mathbf{s}}' d\xi \\ \mathbf{A} &= \rho_s \kappa \oint \mathbf{s} \times \mathbf{s} \times \hat{\mathbf{s}}' d\xi. \end{aligned} \quad (6)$$

Our method of making a reconnection is similar to the ones used by other authors^{8,12–14}. The traditional method is to reconnect vortices as soon as any two points become closer than some critical distance. This critical distance is typically taken to be of the order of the resolution. We calculate, not only the distances between the different vortex points, but keep track on the minimum distance between the vortex segments. (Between neighboring points the vortex is assumed to be straight, standard assumption made within the filament model.) This distance can be smaller than the distance between the points only, and is more accurate if one would use more adaptive point separation where the maximum distance between the points is allowed to grow if the local radius of curvature is large.

In these simulations the point separation is not adaptive, but is simply kept between $\Delta\xi_{\text{res}}/2 < \Delta\xi < \Delta\xi_{\text{res}}$ and the reconnection is done if any two segments are closer than $0.4\Delta\xi_{\text{res}}$, provided that the vortex length decreases in the reconnection event. The same restriction is also used by others. This approximately corresponds that the energy must decrease. Numerically, this might not be visible in E (see e.g. the peak in Fig. 1) since the large curvatures and small distances complicate the accurate calculation of E . The reason for avoiding the adaptive point adjustment, even if it would speed up the simulations, is to minimize the numerical errors: always when a point is added/removed energy is changed by a small amount. Naturally, this error could be totally eliminated by developing an energy conserving algorithm for adding/removing points.

One should note that having a numerical scheme where the energy is too well conserved, might result a numerical bottleneck near the resolution limit. This bottleneck would appear if the cascade from large scales to scales that cannot be resolved is important. It would appear as fractalization of the vortex configuration with characteristic curvatures being of order the numerical resolution. This is not the case here. Even the calculations at zero temperature do not show any signs of accumulation of smallest scale structures, indicating that the Kelvin-wave cascade is not triggered by a single reconnection event, or that the cascade is much too small to be observed (in accordance with Baggaley & Barenghi¹⁵, but in contrast to observations by Kivotides *et al.*¹⁶).

III. RESULTS

Our starting configuration is two linked vortex rings, with radius $R = 1$ mm, and which are separated by a distance of $d_0 = 0.1R$. The vortex rings are oriented such that the initial angle between them is 90° . The initial configuration, together with time development at $T = 0$ (where $\alpha = \alpha' = 0$), is illustrated in Fig. 1. Using closed loops additionally enables us to conveniently evaluate the energy related to vortices by simply using the line-integration formulas, Eq. (6). The bottom part of Fig. 1 illustrates that the energy, linear and angular momentum are well conserved in simulations and that the typical numerical error in energy, or in (angular) momentum is smaller than 0.1%. This implies that our numerical error is well below the total losses appearing in our finite temperature simulations. At finite temperatures the noise is actually smaller than in the zero temperature calculations, because mutual friction tends to stabilize numerics. Figure 1 also shows that the length is only an approximation for the energy and is not necessary constant at zero temperature.

The most important observation obtained from the finite temperature simulations, where $\alpha > 0$, is that even if the energy dissipation is strongly increased by the Kelvin waves appearing immediately after the reconnection, the momentum and angular momentum dissipation are barely affected. This is illustrated in Fig. 2, where the inset shows the time development of the energy, E , momentum, P , and angular momentum, A , when $\alpha = 0.01$. In the main figure we have plotted the time derivatives, $P_{\text{mf}} = dE/dt$, dP/dt , and dA/dt (scaled by their

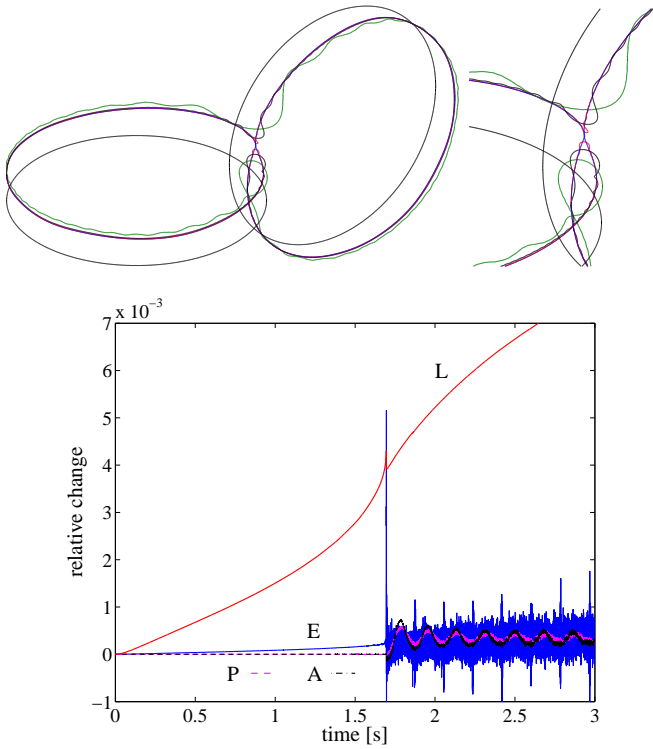


FIG. 1. (Color online) Vortex reconnection at $T = 0$. *Top* panels illustrate the vortex configurations at $t = 0$ (black), 1.695 (blue, just before reconnection), 1.70 (red), 1.75 (black), and 2.00 (green) seconds. The *bottom* panel illustrates the conservation of energy, E , momentum, P , and angular momentum, A , in numerical simulations together with changes in vortex length, L . Vortex reconnection occurs at $t = 1.695$ s, which is seen in the small drop of the vortex length together with a spike in the energy that is due to numerical algorithm used for reconnections. The resolution used here is $\Delta\xi_{\text{res}} = 0.0050$ mm.

values at $t = 0$), using different values for α . As one can note, only the energy dissipation is strongly increased. The dissipation for A is barely affected by the reconnection and for P the dissipation is slightly decreased. The fast fluctuations near $t = t_{\text{rec}}$ are likely due to numerics since they are more sensitive to the resolution, while the overall behavior is not.

The explanation for the weak dissipation of the momentum is the following: The sharp kink induced by the reconnection induces Kelvin waves, but due to conservation of linear and angular momentum the Kelvin waves on different side of the kink must have opposite helicity (k -vector of the Kelvin waves is directed away from the kink). Even if the change in momentum is finite on both sides on the original kink, the total change of the momentum is zero because the changes have opposite signs. Now that the mutual friction starts to damp the Kelvin-waves, the changes in momentum have opposite signs on different regions. However, both sides contribute equally (with positive sign) to the energy dissipation, which is therefore large, compared to the total momentum dissipation.

The strong increase only in the energy dissipation should be valid more generally. It would indicate that in vortex tangles the effective dissipation for the energy can be much larger

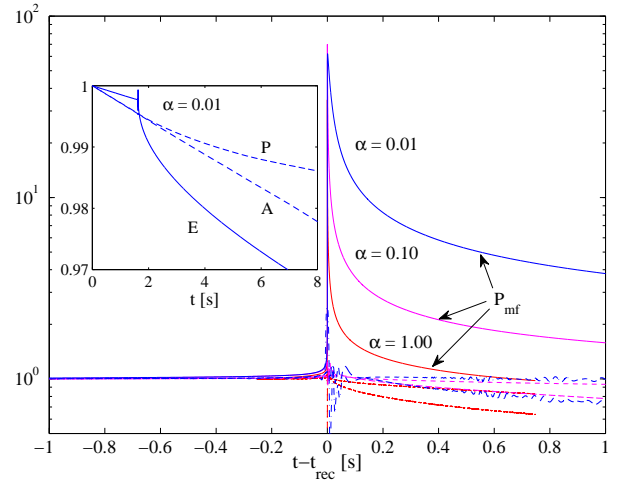


FIG. 2. (Color online) *Inset*: Time development of energy, E , momentum, P , and angular momentum, A , when $\alpha = 0.01$ and $\alpha' = 0$. The values are divided by the initial values at $t = 0$. *Main figure*: Dissipation rate for energy, $P_{\text{mf}} = dE/dt$ (solid lines), momentum dP/dt (dashed) and angular momentum dA/dt (dash-dotted). The rates are again scaled by their respective values at $t = 0$. The three different colors indicate the different values for α : 1 (red), 0.1 (magenta), and 0.01 (blue). Note the logarithmic y-scale.

than the dissipation for the angular momentum. Actually, this effect is recently seen in $^3\text{He-B}$ experiments with propagating turbulent vortex front^{17,18}. In the zero temperature limit the front velocity is observed to saturate, being much larger than the laminar extrapolation. However, the dissipation of the angular momentum is observed to occur much more slowly, the rate approximately given by the laminar estimate *i.e.* m.f. coefficient α .

The poor dissipation of the angular momentum, might also explain why the spin-down of the vortex array in superfluid $^3\text{He-B}$, even at low temperatures, occurs in laminar fashion¹⁹. Turbulence, and much faster decay of the energy, is prevented by the conservation (or more precisely, much slower decay) of the angular momentum. Also, by introducing an additional torque on vortices, *e.g.* by having an extra AB-phase boundary, is observed to increase dissipation²⁰. In superfluid ^4He pinning is important and this may explain why the low temperature behavior is almost always considered to be turbulent. In the remaining part of the paper we try to evaluate, more quantitatively, the energy dissipation coming from a single reconnection event.

The largest problem in evaluating the extra dissipation due to mutual friction originates from estimation of the dissipation without the reconnection disturbance. Especially the asymptotic behavior after the reconnection is somewhat difficult to estimate properly. Well before the reconnection, dissipation comes from shrinking of two independent vortex rings and here the analytical estimation gives a rather good approximation. However, the late time asymptotic after the reconnection is more difficult. At some point the configuration is closer to a single vortex ring, with somewhat larger radius than the initial ones, which eventually shrinks away. (Note that during these

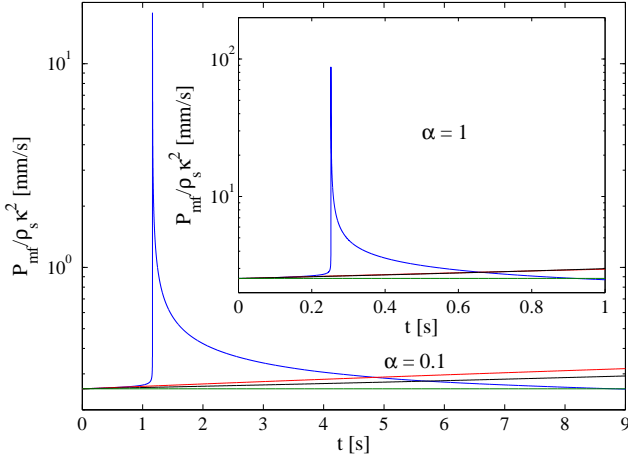


FIG. 3. (Color online) Mutual friction dissipation (blue) together with three different estimations for the laminar background dissipation: linear extrapolation (red, largest), analytical estimation for two independent rings (black), and constant approximation (green, smallest). The *main figure* is for $\alpha = 0.1$, and the *inset* is for $\alpha = 1$.

simulations the total length has dropped 20%, or less.) In the following we make use of the fact that the timescale related to simple shrinking of two initial rings (or the final perturbed ring) is much larger than the timescales related to decay of those small scale structures (Kelvin waves) induced by the reconnection event.

In evaluating the extra dissipation we have used three different methods to estimate the “background” dissipation. All these should overestimate the “true” dissipation. First and the largest estimation is a linear extrapolation before the reconnection. Second estimation comes from analytical estimation of two independent vortex rings with small, of order 3%, adjustment to correctly capture the initial dissipation. The third and the smallest estimation for the background dissipation is simply a constant dissipation taken from the initial value, $P_{mf}(0)$. All these estimations, which are illustrated in Fig. 3, should give the lower limit for the extra dissipation due to the reconnection because at later times the dissipation drops below these estimates. Also, the finite resolution underestimates the dissipation in the vicinity of the reconnection event, where the maximum curvatures are of the order of our resolution.

Our simulations with different α indicate that the power dissipation takes a rather universal form, which can be obtained by scaling the times with α and the m.f. power with $1/\alpha$. In other words the mutual friction dissipation power seems to be given by $P_{mf} = \alpha f(\alpha t)$, with some function $f(x)$. The prefactor comes quite naturally from Eq. (5), but the remaining dependence on αt only must be approximate, but can be attributed to the decay of independent Kelvin-waves whose amplitudes decay exponentially, the timescale being proportional to $1/\alpha$.

The approximate scaling is illustrated in Fig. 4, where we have plotted the scaled dissipation using several values of α , and with different resolutions. In the inset of Fig. 4 the extra dissipation is plotted in case of $\alpha = 0.01$ for five different resolutions (for the two highest resolution the initial configu-

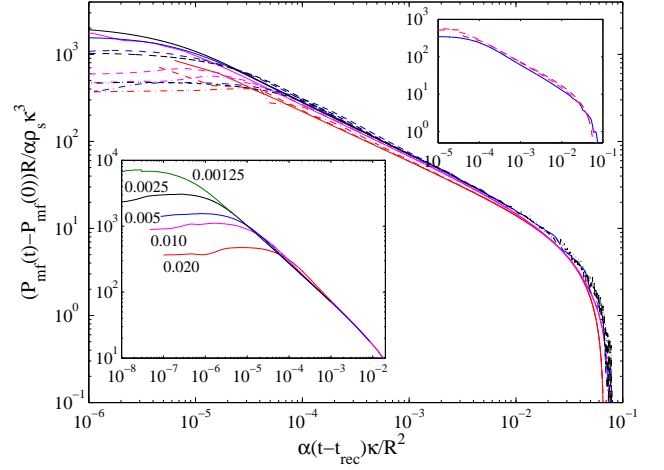


FIG. 4. (Color online) Scaled extra mutual friction dissipation power after the reconnection event. The *main panel* illustrates the results when $R = 1$ mm with four different values of α : 1 (red), 0.1 (magenta), 0.01 (blue), and 0.001 (black), and with three different resolutions: $\Delta \xi_{res} = 0.020$ mm (dash-dotted), 0.010 mm (dashed), and 0.005 mm (solid). In the *lower inset* the extra dissipation with $\alpha = 0.01$ is plotted with five different resolutions. The two additional resolutions (compared with the main panel) are 0.0025 and 0.00125 mm. The *upper inset* illustrates the results with different initial ring radius: $R = 0.1$ mm (blue, solid line), $R = 1.0$ mm (magenta, dash-dotted), $R = 10$ mm (red, dashed), using a resolution of $\Delta \xi_{res}/R = 0.020$, and with $\alpha = 0.01, 0.10$ and 1.00 , respectively.

ration was taken from lower resolution runs, slightly before the reconnection event). Even though the maximum dissipation just after reconnection increases steadily with resolution, the integrated dissipation is almost invariant of the resolution. This is because at intermediate times the higher resolution dissipation drops below the lower resolution results. The large time asymptotics being very similar. After the reconnection, there exist a wide range of timescales where the dissipation function takes a form $f(x) = Ax^{-\gamma}$ with $\gamma \approx 0.6$. The large time behavior (region, where the curves bend strongly down in Fig. 4) is sensitive to the approximation made for the background dissipation, but is consistent with the largest scale Kelvin waves damping exponentially.

At high resolutions and with small mutual friction it becomes numerically too challenging to sweep the same time window $\Delta t/\alpha$, than what is required at high mutual friction and at low resolution to capture all the required dissipation process. In order to be able to compare different simulations more quantitatively, by using computationally more convenient time windows, we define the following energy:

$$E_\tau = \int_{t=0}^{\tau/\alpha} [P_{mf}(t_{rec} + t) - P_{mf}(0)] dt. \quad (7)$$

Here we have used constant approximation for the background, but for $\tau \ll 1$ all three approximations used here give values that differ only by few percents. The total extra dissipated energy, E_{rec} , is obtained when the time integration extends the whole region where $P_{mf}(t) > P_{mf}^{appr}(t)$. In case of constant approximation $P_{mf}^{appr}(t) = P_{mf}(0)$, used in Eq. (7), this

α	$\Delta\xi_{\text{res}}$	t_{max}	t_{rec}	$E_{\text{rec}}^{\text{linear}}$	$E_{\text{rec}}^{\text{anal}}$	$E_{\text{rec}}^{\text{const}}$	$E_{\tau=0.01}$
1.0	0.0200	1.0	0.24980	0.4857	0.4900	0.6072	0.1259
	0.0100	1.0	0.25155	0.4820	0.4867	0.6041	0.1253
	0.0050	1.0	0.25224	0.4819	0.4867	0.6042	0.1260
0.1	0.0200	10	1.15590	0.5172	0.5630	0.6573	0.1490
	0.0100	10	1.16145	0.5088	0.5547	0.6489	0.1440
	0.0050	9.0	1.16300	0.5161	0.5620	0.6562	0.1521
0.01	0.0200	100	1.61360	0.4345	0.6335	0.7123	0.1566
	0.0100	85	1.62255	0.4363	0.6346	0.7131	0.1626
	0.0050	10	1.62481	-	-	-	0.1607
	0.0025 ¹⁾	2.63	1.62512	-	-	-	0.1624
	0.0013 ²⁾	1.63	1.62519	-	-	-	-
0.001	0.0200	800	1.67860	0.2506	0.6294	0.7088	0.1491
	0.0100	60	1.68638	0.2637	-	-	0.1627
	0.0050	12	1.68813	-	-	-	0.1641
0.000	0.0100	2.0	1.69323	-	-	-	-
	0.0050	3.0	1.69514	-	-	-	-

TABLE I. Characteristic numbers from simulations at different α and with different resolutions $\Delta\xi_{\text{res}}$ when the initial configuration is two linked rings with $R = 1$ mm and initial separation of 0.1 mm. Here t_{max} is maximum time reached in our simulations and t_{rec} is the observed reconnection time. Term $E_{\text{rec}}^{\text{appr}}$ is our estimation for the extra dissipation induced by the reconnection event using an approximation “*appr*” for the background dissipation (see text for details). Energy E_{τ} , defined by Eq. (7), indicates the extra energy dissipated during time $\Delta t = \tau/\alpha$ after the reconnection, using a constant approximation for the background. All the lengths are measured in mm’s and the times are in seconds. Energies are scaled by $\rho_s \kappa^2$, which implies that they are also in units of mm’s. For ¹⁾ the starting configuration is taken from the lower resolution run $\Delta\xi_{\text{res}} = 0.0050$ mm at $t = 1.60$ s. For ²⁾ the initial configuration is taken from the run done at resolution $\Delta\xi = 0.0025$ mm at time $t = 1.62$ s.

corresponds to a window where $\tau \approx 0.8$.

The observed scaling law for the mutual friction dissipation also indicates that the Kelvin wave cascade is not important here. If the Kelvin cascade would become dominant at some α , then the cascade would transfer energy to smaller scales, where it would be damped more effectively by m.f., breaking the observed scaling law. Either the single reconnection event is not enough to initialize it (as argued already in Ref. 15), or the amount of mutual friction is still too high, such that the cascade is not resolved. Or, the finite size effects limit the cascade, such that it is not developed. Naturally, the small increase in $E_{\tau=0.01}$ at smaller α ’s might be an indication that Kelvin cascade is raising it’s head. However, since this increase is smaller than errors coming from the estimation of background dissipation, such conclusion is unjustified.

The extra mutual friction dissipation, E_{rec} , induced by the reconnection is rather independent of resolution and depends only weakly on α , as can be seen from Table I. Actually, the value for E_{rec} is more sensitive to the approximation used for the background dissipation than for the value α itself. The value for $E_{\text{rec}}/\rho_s \kappa^2$ is about 0.5 mm. The energy per unit length for straight vortex is $\rho_s \kappa^2 \ln(\ell/a)/(4\pi) \approx \rho_s \kappa^2$, where

ℓ is some cut-off, typically taken as intervortex distance, or system size. Therefore, the dissipation corresponds to decrease of length by about 0.5 mm. This is a rather big value. For example, the estimation for the energy released by sound emission, using the Gross-Pitaevskii equation, corresponds to decrease in length by few coherence lengths only²¹.

One should note that so far we have considered only a reconnection of two vortex rings with initial radius of 1 mm. Since the mutual friction works at every point on the vortex, where the Kelvin waves are rapidly distributed, the total energy must depend on the size of the initial rings. This is verified by repeating the calculations with rings of initial radii of 0.1 mm and 10 mm (see also Fig. 4). In these cases the dissipated energy is about ten times smaller and larger, respectively. This is well consistent with the approximate scaling satisfied by Eq. (3), as noted by Schwarz⁸: If lengths are scaled by a factor λ , times by λ^2 and velocities by $1/\lambda$ then the motion is self-similar. Only the weakly changing logarithmic term (local term) breaks this scaling. The above indicates that the extra dissipated energy corresponds to about few percent of the vortex length, independent of initial ring size.

In real vortex tangles, with lot of reconnections, the time window for the above energy dissipation is likely to be limited by the time between two reconnections occurring within some characteristic distance (e.g. intervortex distance). Similarly, the length, where the dissipation occurs might be (but not necessarily) limited by the intervortex distance. All this complicates the task in evaluating the reconnection induced dissipation in more complicated vortex tangles, but the above values should clearly indicate that, at least with not too small α , the extra dissipation due to mutual friction can be much larger than the previous estimates coming from the sound emission.

Our simulations also confirm the previous filament model calculations and experimental observations that the minimum distance between the vortices behave approximately as $d_{\text{min}} = A\sqrt{\kappa|t - t_{\text{rec}}|}$ both before and after the reconnection^{22–25}. This is shown in Fig. 5. In our case the prefactor A is about ten times bigger after the reconnection than before, reflecting the larger curvatures appearing on the vortex. In classical fluids and in calculations using the Gross-Pitaevskii equation the reconnection is observed to be time asymmetric: $d_{\text{min}} = A|t - t_{\text{rec}}|^\beta$, where β has different value before and after the reconnection^{24,26}.

Also, by simply looking at the vortex configuration, one could qualitative argue that a reconnection event induces an inverse Kelvin-wave cascade. Kelvin waves immediately after the reconnection are at small scales, while at somewhat later time they have much larger amplitude and wavelength. This is consistent with ideas presented by Svistunov about the relaxation of the vortex angle¹. However, the accurate identification of the Kelvin waves on a nontrivial configuration, is not a simple task and can result in unexpected errors²⁷. This results from the fact that generally the Kelvin waves are not well defined except in case of straight vortex or a simple ring. Therefore we have not tried to identify Kelvin waves more quantitatively.

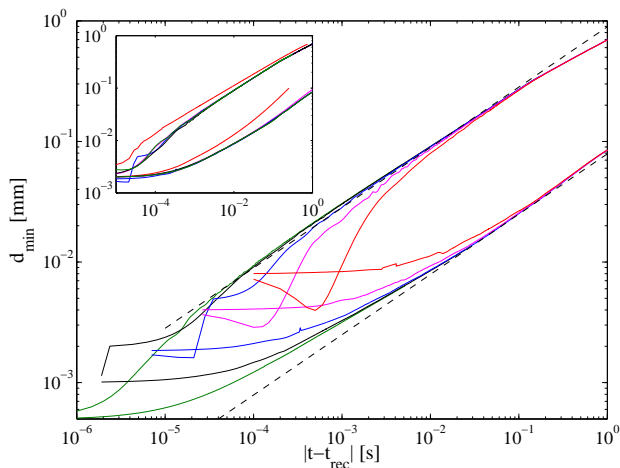


FIG. 5. (Color online) Minimum distance observed in the reconnection event. The lower group of curves describe the times before the reconnections and the upper ones the behavior after the reconnection. The *main figure* illustrates the distance when $\alpha = 0.01$ using five different resolutions: $\Delta\xi_{res} = 0.020$ mm (red), 0.010 mm (magenta), 0.005 mm (blue), 0.0025 mm (black), and 0.00125 mm (green). The dashed lines are guides to the eye such that for $t < t_{rec}$, $d_{min} = \sqrt{\kappa(t_{rec} - t)/16}$, and for $t > t_{rec}$, $d_{min} = \sqrt{8\kappa(t - t_{rec})}$. In the *inset* we have the results using the resolution of $\Delta\xi_{res} = 0.005$ mm but with different α 's: 1 (red), 0.1 (magenta), 0.01 (blue), 0.001 (black) and 0.000 (green).

IV. CONCLUSIONS

Our simple case of two reconnecting vortex rings indicates that the Kelvin waves that appear after the reconnection event

are efficient in dissipating energy, but are much less inefficient in dissipating the angular momentum. This is observed in the measurements of the turbulent vortex front at low temperatures, where the front velocity (related to the energy dissipation), is much bigger than the laminar estimate, but the rotation velocity of the vortex array behind the front drops well below the rotation velocity of the cell^{17,18}. This later decoupling from the external rotating reference frame is an indication that at low temperatures the angular momentum dissipation is much smaller than the energy dissipation and might even vanish in the limit of zero temperature, at least if pinning or surface friction is neglected.

Our numerical estimates for the extra mutual friction dissipation indicate that a single reconnect event can dissipate energy that corresponds to a few percent of the vortex length. This is much larger value than estimations coming from the sound emissions²¹. In real vortex tangles dissipation is expected to be smaller, because it is likely limited by the time between reconnections, intervortex distance, polarization etc. In the zero temperature limit the time required for mutual friction to dissipate enough energy diverges. In that limit the Kelvin-wave cascade and emission of sound should become the dominant dissipation mechanism.

ACKNOWLEDGMENTS

This work is supported by the Academy of Finland (grant 218211) and in part by the EU 7th Framework Programme (FP7/2007-2013, grant 228464 Microkelvin). I would also like to thank M. Krusius, V.B. Eltsov, and N. Hietala for useful discussions, and CSC - IT Center for Science Ltd for the allocation of computational resources.

- ¹ B.V. Svistunov, Phys. Rev. B **52**, 3647-3653 (1995).
- ² W.F. Vinen and J.J. Niemela, J. Low Temp. Phys. **128**, 167-231 (2002).
- ³ D.I. Bradley, D.O. Clubb, S.N. Fisher, A.M. Guénault, R.P. Haley, C.J. Matthews, G.R. Pickett, V. Tsepelin, and K. Zaki, Phys. Rev. Lett. **96**, 035301 (2006).
- ⁴ P.M. Walmsley, A.I. Golov, H.E. Hall, A.A. Levchenko, and W.F. Vinen, Phys. Rev. Lett. **99**, 265302 (2007).
- ⁵ E. Kozik and B. Svistunov, Phys. Rev. Lett. **92**, 035301 (2004).
- ⁶ V.S. L'vov and S. Nazarenko, JETP Lett. **91**, 428-434 (2010).
- ⁷ E.B. Sonin, Phys. Rev. B **85**, 104516 (2012).
- ⁸ K. W. Schwarz, Phys. Rev. B **38**, 2398-2417 (1988).
- ⁹ M. Kursu, K. Bajer, and T. Lipniacki, Phys. Rev. B **83**, 014515 (2011).
- ¹⁰ K. W. Schwarz, Phys. Rev. B **31**, 5782-5804 (1985).
- ¹¹ P.G. Saffman, *Vortex dynamics*, (Cambridge University Press, Cambridge, England, 1992).
- ¹² M. Tsubota, T. Araki, S. K. Nemirovskii, Phys. Rev. B **62**, 11751-11762 (2000).
- ¹³ L. P. Kondaurova, V. A. Andryuschenko, and Sergey K. Nemirovskii, J. Low Temp. Phys. **150**, 415-419 (2008).
- ¹⁴ A. W. Baggaley, J. Low Temp. Phys. **168**, 18-30 (2012).
- ¹⁵ A. W. Baggaley, and C. F. Barenghi, Phys. Rev. B **83**, 134509 (2011).
- ¹⁶ D. Kivotides, J.C. Vassilicos, D.C. Samuels, and C.F. Barenghi, Phys. Rev. Lett. **86**, 3080-3083 (2001).
- ¹⁷ J.J. Hosio, V.B. Eltsov, P.J. Heikkinen, R. Hänninen, M. Krusius, and V. S. L'vov Nat. Comm. **4**, 1614 (2013).
- ¹⁸ J.J. Hosio, V.B. Eltsov, R. de Graaf, P.J. Heikkinen, R. Hänninen, M. Krusius, V.S. L'vov, and G.E. Volovik, Phys. Rev. Lett. **107**, 135302 (2011).
- ¹⁹ V.B. Eltsov, R. de Graaf, P.J. Heikkinen, J.J. Hosio, R. Hänninen, M. Krusius, V.S. L'vov, Phys. Rev. Lett. **105**, 125301 (2010).
- ²⁰ P.M. Walmsley, V.B. Eltsov, P.J. Heikkinen, J.J. Hosio, R. Hänninen, and M. Krusius, Phys. Rev. B **84**, 184532 (2011).
- ²¹ M. Leadbeater, T. Winiecki, D.C. Samuels, C.F. Barenghi, and C.S. Adams, Phys. Rev. Lett. **86**, 1410-1413 (2001).
- ²² A.T.A.M. de Waele, and R.G.K.M. Aarts, Phys. Rev. Lett. **72**, 482-485 (1994).
- ²³ M. Tsubota, and H. Adachi, J. Low Temp. Phys. **162**, 367-374 (2011).
- ²⁴ S. Zuccher, M. Caliar, A. W. Baggaley, and C.F. Barenghi, Phys. Fluids **24**, 125108 (2012).
- ²⁵ M. S. Paoletti, M. E. Fisher, K. R. Sreenivasan, and D. P. Lathrop, Phys. Rev. Lett. **101**, 154501 (2008).
- ²⁶ F. Hussain and K. Duraisamy, Phys. Fluids **23**, 021701, (2011).
- ²⁷ R. Hänninen, and N. Hietala, J. Low Temp. Phys. (2013) doi:10.1007/s10909-012-0749-6; arXiv:1208.5403.